

Surface Plasmon Polariton microscope with Parabolic Reflectors

Aurelien Drezet, Daniel Koller, Andreas Hohenau, Alfred Leitner, Franz R. Aussenegg, and Joachim R. Krenn

*Institute of Physics and Erwin Schrödinger Institute for Nanoscale Research,
Karl-Franzens-University, Universitätsplatz 5, 8010 Graz, Austria*

(Dated: November 3, 2018)

We report the realization of a two-dimensional optical microscope for surface plasmons polaritons (SPPs) based on parabolic Bragg mirrors. These mirrors are built from lithographically fabricated gold nanostructures on gold thin films. We show by direct imaging by leakage radiation microscopy that the magnification power of the SPP microscope follows basic predictions of geometrical optics. Spatial resolution down to the value set by the diffraction limit is demonstrated.

PACS numbers:

Surface plasmon polaritons (SPPs) are propagative electromagnetic waves bound to the interface between a metal and a dielectric [1]. As such, SPPs offer several possibilities for two-dimensional optical functionalities at micro- and nanometer scales [2]. Various quasi two-dimensional SPP elements were demonstrated recently such as waveguides [3–5], lenses [6, 7], reflectors [8, 9] and interferometers [8, 10, 11]. In particular, the realization of an elliptical interferometer for SPPs based on confocal Bragg reflectors built on a flat gold film was reported [10]. In this interferometer SPPs launched from the first focal point F_1 are efficiently focussed in the second focal point F_2 after propagating inside an elliptical cavity. Clearly such a geometry can as well be used for in-plane microscopic imaging [12]. In fact, SPP microscopy has been a topic of increased interest recently, including some controversy about the achievable spatial resolution [13, 14]. For geometrical reasons, however, an elliptical geometry does not allow to obtain an image magnification much different from unity. To overcome this limitation we report here the realization of an SPP in-plane microscope with parabolic mirrors. We realize two-dimensional SPP imaging with variable magnification and show that a spatial resolution of about half the SPP wavelength is attainable in agreement with the Abbe-Rayleigh criterion [15, 16].

All structures discussed in the following are built from gold nanoprotusions (150 nm diameter, 70 nm height) fabricated by standard electron-beam lithography [17] on a 70 nm thick gold thin film on glass substrate. To achieve SPP reflectivity close to unity a Bragg mirror geometry has been chosen for the reflectors constituted by 11 parabola sharing the same focal point (and having thus slightly different focal lengths) and the same symmetry axis. The individual parabola are built from closely spaced protrusions (center-to-center distance ~ 250 nm). Constructive interference occurs between the various reflected and refocussed SPP waves if the closest separation between two neighboring parabola (measured along the symmetry axis) equals $\lambda_{\text{SPP}}/2$, where λ_{SPP} is the SPP wavelength which is here fixed to 785 nm, corresponding to a laser excitation wavelength of 800 nm.

As a first example we consider a confocal geometry composed of two parabolic reflectors having the same focal length and common symmetry axis F_1F_2 (see Fig. 1). The object to be imaged is located close to F_1 . From the geometrical properties of parabola mirrors one can see that the light path $F_1M + MH$ (where M is the effective SPP reflection point on the parabola and H is the horizontal projection of M onto a line perpendicular to the parabola axis, see Fig. 1A) is independent of the choice of the position of M . Clearly this means that F_1 is projected into a SPP beam propagating along F_1F_2 and finally that a SPP launched in F_1 is refocussed in F_2 .

In Fig. 1B the object in F_1 is a single gold nanoprotusion. SPPs are launched on the metal film by focussing on this nanoprotusion a laser beam impinging perpendicularly to the surface with a polarization direction oriented along the vertical direction. The imaging of SPP propagation is accomplished by leakage radiation microscopy (LRM) which relies on the conversion of SPP waves into propagating light through the glass substrate [18–20]. It is clearly visible in the image that efficient SPP refocussing is obtained in F_2 , with an intensity pattern around the focus that corresponds to that in a plane containing the optical axis in conventional microscopy. We note that a large part of the image is saturated due to the limited dynamics of the camera used to capture the LRM images. Figs. 1C and D show LRM images for the case of a protrusion pair as the object in the area of F_1 . Here, the pair axis is aligned along the symmetry axis of the mirrors, i.e., along the horizontal direction and the protrusion distances are $d = 1\mu\text{m}$ (C) and $d = 2\mu\text{m}$ (D), respectively. The insets in Figs. 1B–D show intensity cross-cuts along the symmetry axis around F_2 as marked by the triangles in the images. In both cases the object structure is clearly imaged in F_2 . The measured separations of the image spots correspond to those of the protrusion pairs, directly demonstrating unity longitudinal magnification for the case of identical focal distances of the two parabola.

We now turn to image magnification by using two different parabolic reflectors with focal lengths $f_1 = 5\mu\text{m}$ and $f_2 = 15\mu\text{m}$ (see Fig. 2A). Fig. 2B shows a two-

dimensional dipolar simulation [21] of the expected intensity distribution in the parabolic cavity when SPPs are launched from a single nanoprotusion located at F_1 .

This result reproduces fairly the experimental LRM image corresponding to this configuration, shown in Fig. 2C. As previously reported, in LRM certain SPP components with specific in-plane momentum can be Fourier filtered in the back focal plane of the imaging microscope objective [22]. Thereby these components and according spurious interference can be eliminated from the direct space images, exposing otherwise obstructed features to direct analysis. Fig. 2D zooms a detail of Fig. 2C after filtering all SPP components propagating from right to left. As now only SPPs reflected by the second (left) mirror, i.e., propagating from left to right contribute to the image we recover a clear image of the focal region.

For demonstrating microscopic magnification we now analyze the transverse magnification of our SPP in-plane microscope [12] which is simply given by $f_2/f_1 = 3$. We therefore consider again nanoprotusion pairs located near F_1 . While the position of one protrusion is in F_1 , the second protrusion is separated by a distance along the direction perpendicular to the microscope symmetry axis of $d' = 2, 1$ and $0.4 \mu\text{m}$ (see Fig. 3). The according LRM images are shown in Figs. 3A, C and E which again display Fourier filtered images, suppressing all SPP components propagating from right to left.

The images of the two protrusion are clearly visible and resolved, even for the smallest distance $d' = 0.4 \mu\text{m} \simeq \lambda_{\text{SPP}}/2$. Using the filtered LRM images we obtain transverse cross-cuts of the SPP intensity along the line joining the centers of the two image points, see panels B, D and F of Fig. 4. To guide the eye we include Gaussian fits to the data. Clearly the image of the off-axis protrusion is broader than that of the on-axis protrusion which is due to aberration. Most importantly, however, the observed distances between the image spots are a factor of 3 larger than the distances between the nanoprotusions, thus directly evidencing the expected factor for the transverse magnification as expected from geometrical optics.

To conclude, we have experimentally demonstrated an in-plane SPP microscope relying on parabolic Bragg mirrors with a spatial resolution of about $\lambda_{\text{SPP}}/2$. In the context of plasmonics this microscopic scheme could complement existing elements as waveguides, mirrors, etc., for the benefit of applications in SPP based imaging, optical sub-wavelength addressing or sensing.

- [4] T. Nikolajsen, K. Leosson, I. Salakhutdinov, and S. I. Bozhevolnyi, *Appl. Phys. Lett.* **82**, 668 (2003).
- [5] H. Ditlbacher, A. Hohenau, D. Wagner, U. Kreibig, M. Rogers, F. Hofer, F. R. Aussenegg, J. R. Krenn, *Phys. Rev. Lett.* **95**, 257403 (2005).
- [6] A. Hohenau, J. R. Krenn, H. Ditlbacher, A. Hohenau, A. Drezet, B. Steinberger, A. Leitner, and F. Aussenegg, *Opt. Lett.* **30**, 893 (2005).
- [7] Z. Liu, J. M. Steele, W. Srituravanich, Y. Pikus, C. Sun, and X. Zhang, *Nano Lett.* **5**, 1726 (2005).
- [8] H. Ditlbacher, J. R. Krenn, G. Schider, A. Leitner, and F. R. Aussenegg, *Appl. Phys. Lett.* **81**, 1762 (2002).
- [9] L. Yin, V. K. Vlasko-Vlasov, J. Pearson, J. M. Hiller, J. Hua, U. Welp, D. E. Brown, and C. W. Kimball, *Nano Lett.* **5**, 1399 (2005).
- [10] A. Drezet, A. L. Stepanov, H. Ditlbacher, A. Hohenau, B. Steinberger, F. R. Aussenegg, A. Leitner, and J. R. Krenn, *Appl. Phys. Lett.* **86**, 074104 (2005).
- [11] S. I. Bozhevolnyi, V. S. Volkov, E. Deveaux, J. Y. Laluet, and T. W. Ebbesen, *Nature* **440**, 508 (2006).
- [12] By analogy with classical (three-dimensional) optical microscopes which are adapted for imaging of two-dimensional systems located in the object plane, a two-dimensional optical microscope is only able to image one-dimensional systems located along the *object line* perpendicularly to the optical axis. This limitation is accepted in the present article.
- [13] I. I. Smolyaninov, J. Elliott, A. V. Zayats, C. Davis, *Phys. Rev. Lett.* **94**, 057401 (2005).
- [14] A. Drezet, A. Hohenau, and J. R. Krenn, *Phys. Rev. Lett.* **98**, 209703 (2007).
- [15] M. Born and E. Wolf, *Principles of Optics, seventh (expanded) edition* (Cambridge University Press, Cambridge, 1999).
- [16] A. Drezet, A. L. Stepanov, A. Hohenau, B. Steinberger, N. Galler, H. Ditlbacher, A. Leitner, F. R. Aussenegg, J. R. Krenn, M. U. Gonzalez, J.-C. Weeber, *Euro. Phys. Lett.* **74**, 693 (2006).
- [17] M. A. McCord and M. J. Rooks, in *Handbook of Microlithography, Micromachining and Microfabrication, Volume 1* edited by P. Rai-Choudhury (SPIE and The Institution of Electrical Engineers, Bellingham, Washington, 1997), pp. 139-249.
- [18] B. Hecht, H. Bielefeldt, L. Novotny, Y. Inouye, and D. W. Pohl, *Phys. Rev. Lett.* **77**, 1889 (1996).
- [19] A. Bouhelier, Th. Huser, H. Tamaru, H. -J. Güntherodt, D. W. Pohl, Fadi I. Baida and D. Van Labeke, *Phys. Rev. B* **63**, 155404 (2001).
- [20] A. Stepanov, J. R. Krenn, H. Ditlbacher, A. Hohenau, A. Drezet, B. Steinberger, A. Leitner, and F. Aussenegg, *Opt. Lett.* **30**, 1524 (2005).
- [21] H. Ditlbacher, Ph.D. Thesis, Karl-Franzens University Graz (2003).
- [22] A. Drezet, A. Hohenau, A. Stepanov, H. Ditlbacher, B. Steinberger, N. Galler, F. R. Aussenegg, A. Leitner, J. R. Krenn, *Appl. Phys. Lett.* **89**, 091117 (2006).

-
- [1] H. Raether, *Surface Plasmons* (Springer, Berlin, 1988).
 - [2] W. L. Barnes, A. Dereux, T. W. Ebbesen, *Nature* **424**, 824 (2003).
 - [3] J. C. Weeber, Y. Lacroute, and A. Dereux, *Phys. Rev. B* **68**, 115401 (2003).

Figure: 1//

Confocal parabolic SPP microscope. (A) Scanning electron microscope image. F_1 and F_2 are the focal points, the focal distances are $f_1 = f_2 = 15\mu\text{m}$ and the lines show exemplary SPP paths from F_1 to F_2 . The inset displays a magnified image of the nanoprotusions constituting the Bragg mirror structure. The minimum separation between two adjacent mirrors is $a = \lambda_{\text{SPP}}/2 = 390\text{nm}$. (B) LRM image with a single nanoprotusion at F_1 . The laser polarization is indicated by the double arrow. (C) Same as (B) but with a protrusion pair separated by a horizontal distance $d = 1\mu\text{m}$. (D) Same as (B) but with a protrusion pair separated by a horizontal distance $d = 2\mu\text{m}$. The insets in (B)–(D) show cross-cuts of the SPP intensity along the symmetry axis near F_2 , as indicated by the triangles in the images. The cross-cut scale bar is $2\mu\text{m}$, the vertical lines are separated by $d=1\mu\text{m}$ (C) and $2\mu\text{m}$ (D).

Figure 2: //

Magnifying parabolic SPP microscope. (A) Scanning electron microscope image. (B) Two-dimensional dipolar simulation of SPPs propagating inside the parabolic mirrors after launching from F_1 . The laser polarization direction is indicated by the double arrow. (C) LRM image corresponding to (B). (D) Magnified LRM image corresponding to the dashed white rectangle in (C) after Fourier filtering of the SPP components propagating from left to right.

Figure 3: //

Microscopic imaging of a nanoprotusion pair located near F_1 using the geometry shown in Fig. 2. A, C and E show the Fourier filtered LRM images for pairs (SEM images shown in the insets) separated by $d = 2, 1$ and $0.4\mu\text{m}$, respectively. The images cover areas corresponding to the same dashed rectangles as in Fig. 2C. B, D, and F show LRM intensity cross-cuts taken along the dashed lines of images A, C and E, respectively. The curves are Gaussian fits to the data.

Figure 1://

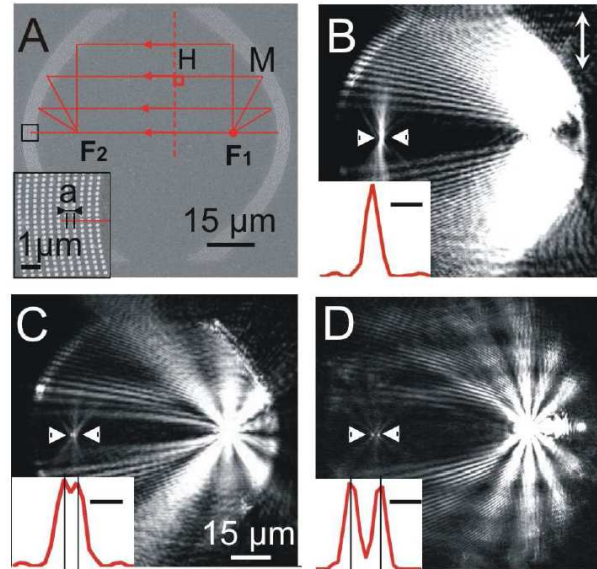


FIG. 1:

Figure 2://

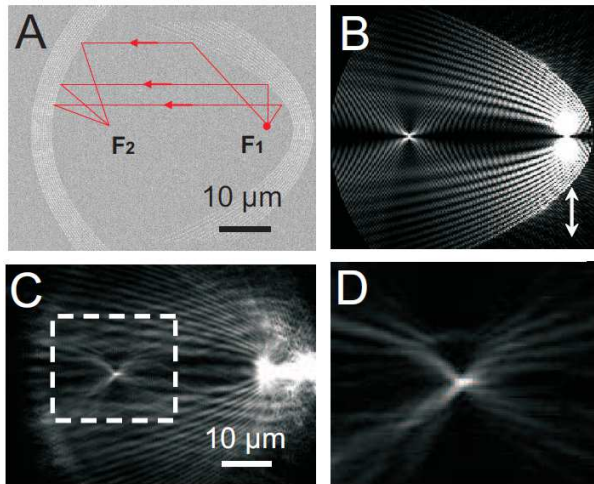


FIG. 2:

Figure 3://

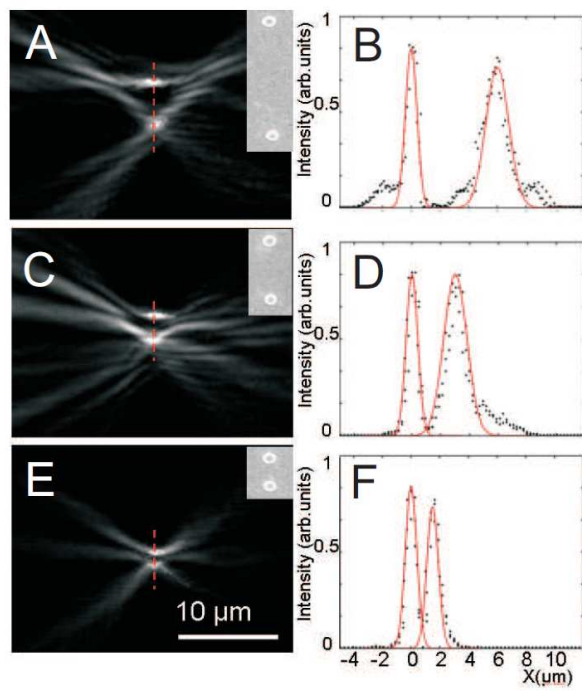


FIG. 3: